

INFLAMMATION ARISING FROM OBESITY REDUCES TASTE BUD ABUNDANCE
AND RENEWAL

A Dissertation

Presented to the Faculty of the Graduate School
of Cornell University

In Partial Fulfillment of the Requirements for the Degree of
Doctor of Philosophy

by

Andrew Kaufman

January, 2017

© 2017 Andrew Kaufman

INFLAMMATION ARISING FROM OBESITY REDUCES TASTE BUD ABUNDANCE
AND RENEWAL

Andrew Kaufman, Ph. D.

Cornell University 2017

Despite evidence that the ability to taste is weakened by obesity and rescued with weight loss intervention, few studies have investigated the molecular effects of obesity on the physiology of taste. Taste bud cells undergo continual turnover, even in adulthood, exhibiting an average life span of about 10 days, tightly controlled by a balance of proliferation and cell death. Recent data reveal that an acute inflammation event can upset this balance. I demonstrate that chronic low-grade inflammation brought on by an obesogenic diet reduces the number of taste buds in gustatory tissues of mice, by attenuating the renewal of taste cells, and is likely the cause of taste dysfunction seen in obese populations.

BIOGRAPHICAL SKETCH

Andrew Kaufman received his Bachelor of Arts degree in Biochemistry from Columbia University in 2008, where he also was a member of Dr. Elizabeth Miller's cell biology research group. While at Columbia, he learned to use yeast as a model system to understand protein trafficking and folding mechanisms involved in disease progression, Cystic Fibrosis in particular.

Upon graduation, Andrew went on to work at Memorial Sloan Kettering Cancer Center as a research technician, where he collaborated with medical oncologist Dr. Timothy Chan and the hospital's surgical staff to identify and characterize novel tumor suppressor genes involved in breast, colorectal, and head and neck cancers.

Andrew returned to Cornell to pursue his PhD in Food Science, where his interest in public health and experience in cell and molecular biology led him to research taste bud development in metabolic disorder. He plans to continue in the field of taste physiology and development at the University of Colorado – Denver Medical School, studying taste disorders in chemotherapy patients.

ACKNOWLEDGMENTS

Grateful thanks to Dr. Xiling Shen of Duke University and Dr. Ling Qi for providing transgenic mouse lines, and for consultation with project design. I also thank the Department of Food Science at Cornell University for funding this project and Dr. Robin Dando for his excellent ideas and guidance.

TABLE OF CONTENTS

Biographical Sketch	iii
Acknowledgements	iv
Table of Contents	v
Introduction	1
HFD induces obesity and increases TNF α in taste	4
Fewer taste buds and taste markers in obese mice	7
Taste stem and progenitor cell loss in obesity	10
Deletion of TNF α protects taste buds from obesity	14
Materials and Methods	22
References	25

CHAPTER 1
INFLAMMATION ARISING FROM OBESITY REDUCES TASTE BUD ABUNDANCE
AND RENEWAL

Introduction

Obesity is one of the world's most important public health problems, affecting over one-third of US citizens¹, and is associated with increased mortality, and co-morbidities including cardiovascular disease, diabetes, stroke, and cancer².

The treatment of obesity presents major challenges, including poor adherence to diet, inadequate weight loss, and high rates of attrition³. Despite many studies outlining the disastrous effects of obesity, people continue to eat unhealthily. Various studies have investigated the relationship between body mass index (BMI) and taste perception, with differing results. Earlier reports suggest little no effect of BMI on taste sensitivity^{4,5}. These studies tested detection thresholds for sweet stimuli in obese and normal-weight humans, but failed to take into account individual variation in the perception of suprathreshold stimuli. With the invention of the generalized Labeled Magnitude Scale (gLMS), intensity ratings could be compared across groups by anchoring the upper end of intensity scales to “strongest imaginable sensation of any kind”, rather than strongest taste sensation, thus negating the possibility that the obese fundamentally perceive taste differently.⁶ Use of the gLMS revealed a negative association between BMI and perceived intensity of sweetness, umami, saltiness, and fatty taste⁷⁻¹⁰. Some researchers have also explored the association between high BMI and decreased dopamine signaling from food intake suggesting that the obese and overweight seek out more palatable foods to compensate for depressed reward^{11,12}. Weight loss interventions, both gradual and acute (i.e. via bariatric

surgery), have proven to alleviate obesity-related alterations in taste function, suggesting a bidirectional relationship between obesity and taste. Gastric bypass surgery in both rodents and humans can reestablish taste thresholds and reward signaling to levels seen in normal-weight controls, as well as decreasing the preference for, and intake of calorie-rich foods^{13–20}. Despite evidence that taste is weakened in obesity and rescued with weight loss intervention, few studies have investigated the molecular effects of obesity on the physiology of the taste system.

A taste bud consists of a heterogeneous collection of 50-100 cells belonging to three functionally independent cell types. Type I cells are glial-like, provide structural support for the taste bud, and are likely responsible for salty taste detection²¹. Type II cells express G-protein-coupled receptors (GPCRs) for sweet, bitter, or umami tastants, and transduce taste signals via the PLC β 2/PIP₂/IP₃ cascade^{22–24}. Type III cells form synapses with afferent nerve fibers, and respond to sour taste^{25,26}. Type II cells release ATP as their primary neurotransmitter, while Type III cells accumulate and release serotonin and synthesize the inhibitory transmitter GABA^{27–29}.

Taste bud cells undergo continual turnover, even into adulthood, exhibiting an average life span of about 10 days³⁰. Recently, a population of lingual stem cells has been identified that give rise to mature taste bud cells in the circumvallate papillae³³. These cells express leucine-rich repeat-containing G-protein coupled receptor 5 (LGR5), which is also expressed by stem cells of the intestinal epithelium. LGR5 has been identified as a receptor for R-spondins, which activate the WNT-signaling pathway^{31–33}. Upon activation of WNT, these low-LGR5-expressing stem cells differentiate into immature SOX2⁺ cells and migrate into the taste bud, losing their LGR5 expression in the process. SOX2 is required for the differentiation of endodermal progenitor cells of the tongue into mature taste bud cells and represents one of the last steps before terminal differentiation³⁴.

There are a number of processes that affect the generation of new functional taste cells from immature progenitor cells. Acute lipopolysaccharide (LPS)-induced inflammation has been shown to inhibit proliferation of taste progenitor cells and reduced the number of newborn cells entering taste buds. Furthermore, LPS-induced inflammation was shown to moderately shorten the average lifespan of mature taste bud cells³⁵. These experiments show the effects of inflammation in short term, acute administration, a relatively rare occurrence. Far more common is the chronic and systemic low-grade inflammation found in obesity, with no research on such a model in taste yet reported. Evidence indicates that a state of low-grade chronic inflammation has a crucial role in the pathogenesis of obesity-related metabolic dysfunction^{36,37}. With increased amounts of visceral adipose tissue, the production of proinflammatory cytokines, including TNF α , IL-6, and CCL2, is upregulated in the obese, with the potential to act on receptors within the taste bud, inducing cell death cascades^{38,39}. TNF α in particular has been well documented as a key mediator of obesity-related pathologies^{36,37,40,41}. This study investigates the effects of low-grade inflammation on the regenerative processes of taste buds in the obese state, demonstrating a biological mechanism for taste dysfunction seen in human sensory studies of obese populations.

HFD induces obesity and increases TNF α in taste

Obesity is associated with a number of comorbidities and pathologies, with many stemming from the increase in circulation of pro-inflammatory cytokines^{36,37}. Acute induction of systemic inflammation via intraperitoneal injection of lipopolysaccharide (LPS) has been demonstrated to shorten the lifespan of adult taste bud cells and reduce the population of supporting progenitor cells³⁵. I split littermates of 8-week old wild-type C57Bl/6 male mice into two cohorts, which were treated with either a standard chow or a high fat diet (HFD) for a period of 8 weeks (Figure 1A).

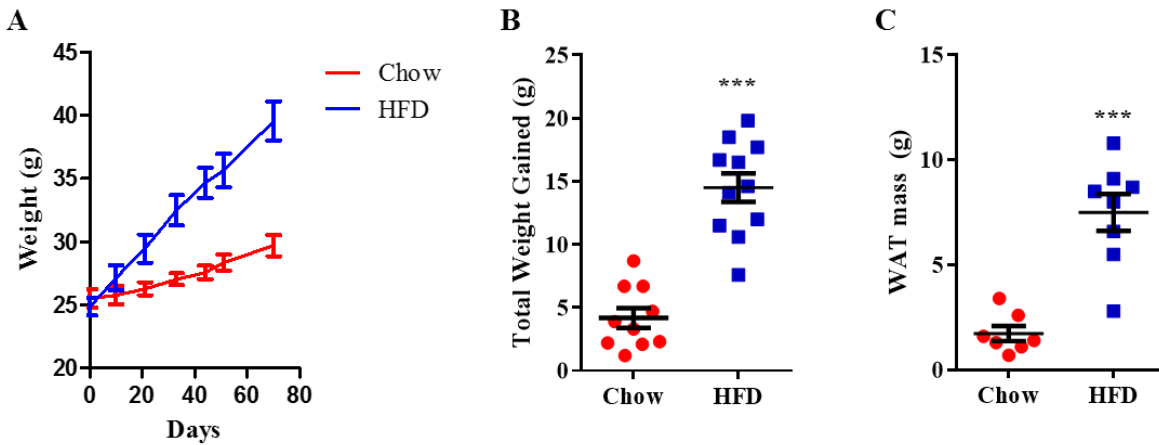


Figure 1. High fat diet induces adipogenesis. (A) Growth curve of C57Bl/6 WT male mice over 8-weeks ad libitum feeding with standard chow and high fat diet (HFD). (B) Total weight gained by WT male mice after 8-week treatment period of standard chow and HFD (n=10, 11, respectively) (C) White adipose tissue (WAT) mass from WT male mice after 8-week treatment period of standard chow and HFD (n=7,8, respectively).

Mice gained significantly more weight when fed the HFD than those fed standard chow (Figure 1B) and post-mortem analysis showed that the majority of weight gained by the HFD-fed mice was in the form of white adipose tissue (Figure 1C). Representative images of the gross anatomy of chow and HFD-fed mice follow below:

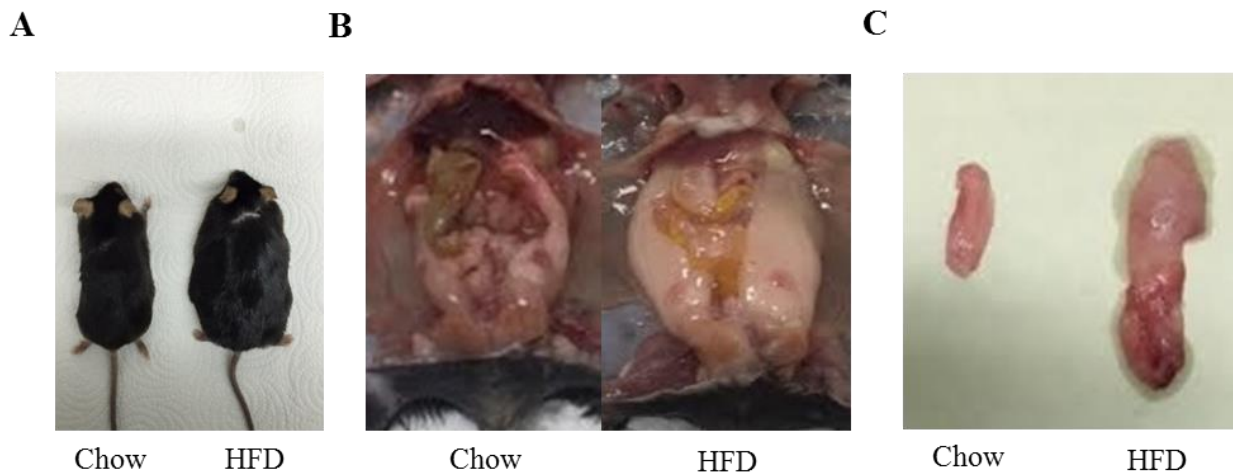


Figure 2: High fat diet induces adipogenesis. (A) Representative picture of chow and HFD-fed WT male mice after 8 weeks. (B) Representative pictures of abdomen from chow and HFD-fed WT male mice after 8 weeks. (C) Representative picture of epididymal fat pads (EF) from chow and HFD-fed WT male mice after 8 weeks.

I then tested whether this was sufficient to induce an inflammatory response associated with increased adiposity. I examined the expression of several inflammatory cytokines, including $\text{TNF}\alpha$, IL-6, and IL-1 β in circumvallate papillae taste buds. Quantitative real-time reverse transcription polymerase chain reaction (qRT-PCR) analysis showed that after only 8 weeks, expression levels of $\text{TNF}\alpha$ were significantly increased (around ten-fold) in HFD-fed mice, compared to lean controls (Figure 3), with only moderate variation in interleukins at this time

point. These results suggest that prolonged obesity can induce a robust-yet-specific inflammatory response in the taste epithelium, consistent with reports localizing components of the inflammatory response to taste buds³⁹.

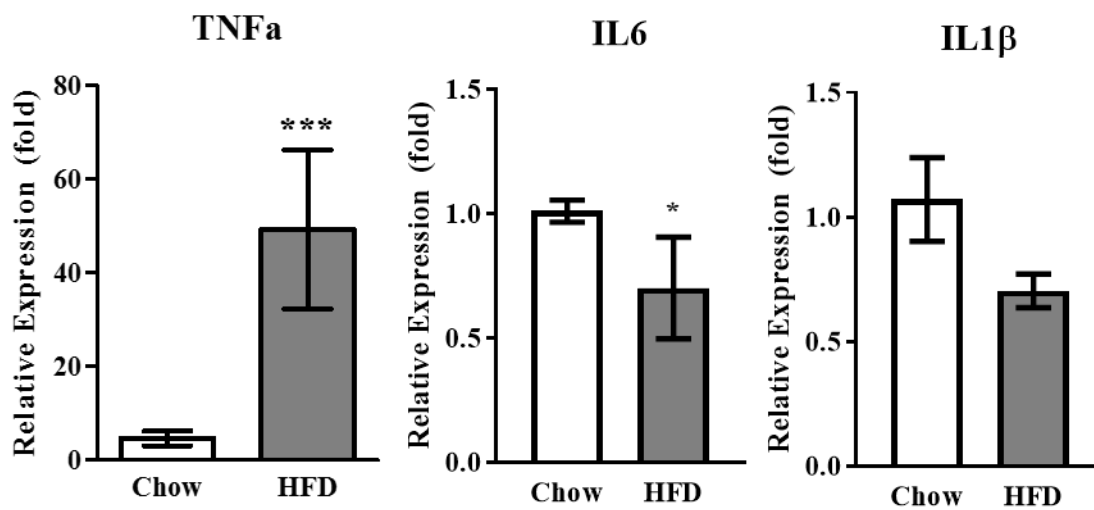


Figure 3: High fat diet increases expression of proinflammatory cytokine TNFα. Quantitative real-time PCR analysis of the expression of inflammatory cytokines in circumvallate papillae (CV) after 8-week treatment with chow and HFD (n=6 each). Relative gene expression levels are shown (fold change). β -actin was used as the endogenous control gene for relative quantification. Error bars represent SEM. * $p < 0.05$; ** $p < 0.01$; *** $p < 0.005$.

Fewer taste buds and taste markers in obese mice

Correlations have previously been reported between taste bud density and perceived taste intensity⁴¹. In order to examine taste deficiency in the obese from a biological standpoint, I first investigated the relative abundance of taste buds in obese mice compared to lean controls. Following the same dietary treatment as previously described, tissue sections containing circumvallate papillae were processed for immunofluorescent staining using antibodies against KCNQ1, a marker for all taste bud cells⁴². Representative immunostaining images from lean and obese mice are shown in Figure 4.

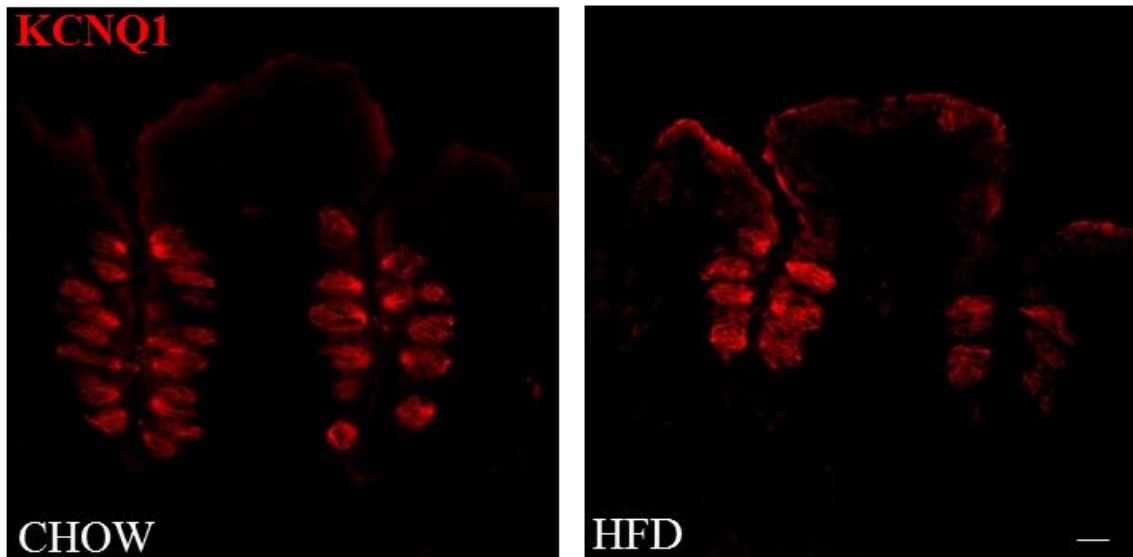


Figure 4: Loss of taste buds in obese WT mice: Fluorescent images of circumvallate papillae sections stained with goat antibody against KCNQ1. AlexaFluor 647-conjugated secondary antibody was used. Scale bars, 50 μ m.

Quantification of total taste bud counts for whole circumvallate papillae revealed a significant reduction in taste bud abundance in obese mice (Figure 5A). While the abundance of taste buds in obese mice declined, no difference in the size of taste buds was evident between lean and obese cohorts (Figure 5B).

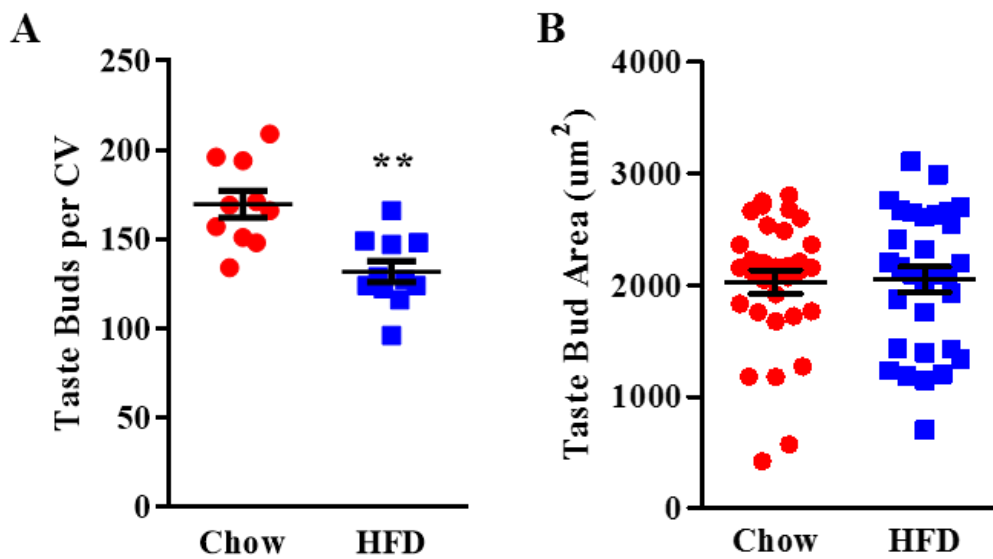


Figure 5: Quantification of taste bud loss in obese WT mice. (A) Total numbers of taste buds in circumvallate papillae of chow and HFD-fed WT male mice after 8 weeks shows a nearly 25% reduction in taste bud abundance in obese mice (n=10, 11, respectively). (B) Taste bud area from chow and HFD-fed WT male mice after 8 weeks reveals no change (n=32, 31, respectively). Error bars represent SEM. * p < 0.05; ** p < 0.01; *** p < 0.005.

Quantitative real-time RT-PCR revealed that the expression of KCNQ1, as well as markers for taste transduction such as PLC β 2, T1R3 and NTPDase2 were significantly decreased in obese mice compared to lean controls (Figure 6), consistent with a recent report on the effects of obesity on extra-oral expression of taste receptors⁴³. These data support the hypothesis that taste dysfunction in the obese originates with a fundamental change in gustatory morphology.

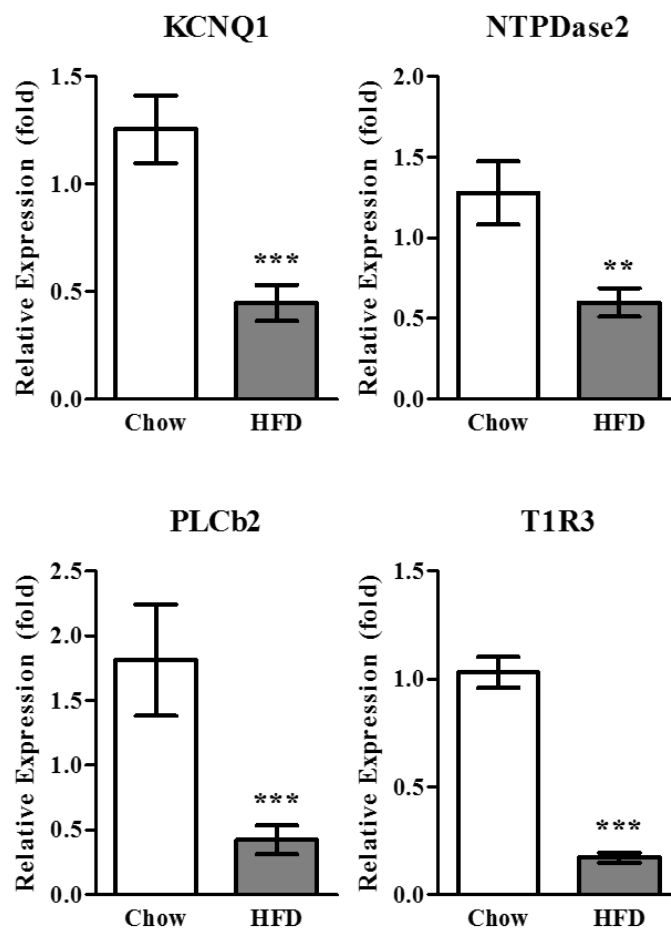


Figure 6: Loss of expression of taste bud machinery in obese WT mice. Quantitative real-time PCR analysis of the expression of taste cell markers in circumvallate papillae (CV) after 8-week treatment with chow and HFD. Relative gene expression levels are shown (fold change). β -actin was used as the endogenous control gene for relative quantification. Error bars represent SEM (n=6 each). * p < 0.05; ** p < 0.01; *** p < 0.005.

Taste stem and progenitor cell loss in obesity

LGR5 has been identified as a marker for stem cell populations in the gustatory epithelium, with single LGR5⁺ cells capable of producing adult taste bud cells ex vivo^{33,44}. In order to examine the effects of diet-induced obesity on the expression of LGR5 in taste stem cell populations, I subjected two cohorts of 8-week old male transgenic mice expressing a fluorescent reporter in LGR5 positive cells to the same dietary treatment previously described. Figure 7 shows representative images of endogenous LGR5 expression in lean and obese LGR5-eGFP mice, consistent with previous reports of LGR5 localization⁴⁵.

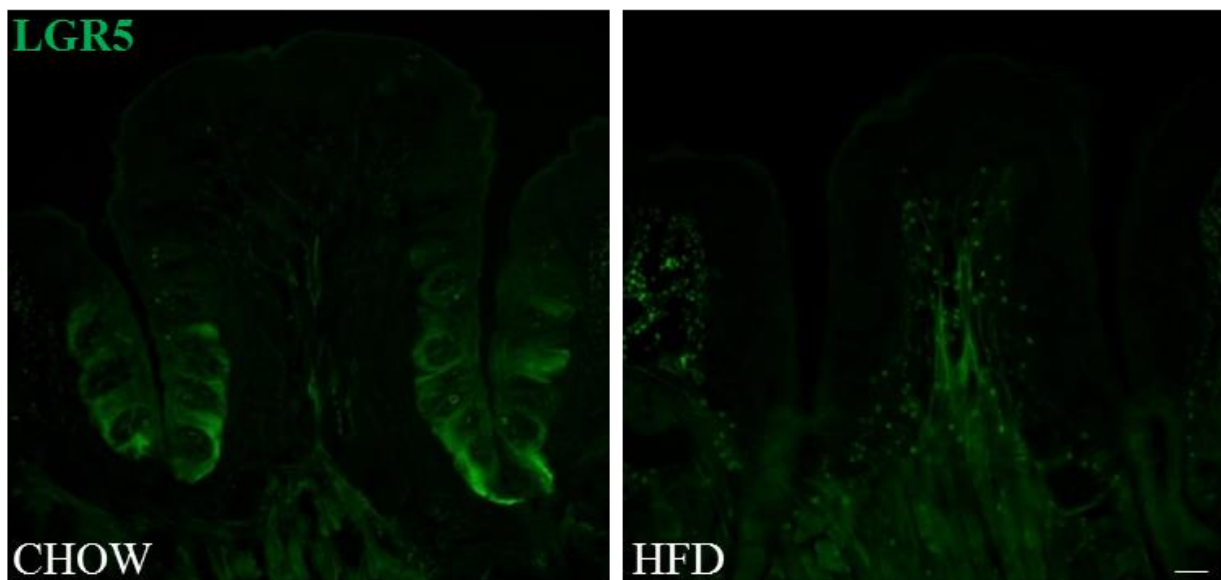


Figure 7: Taste stem cell population loss in obese WT mice. Confocal fluorescent images of GFP-labeled LGR5 from circumvallate papillae of chow and HFD-fed LGR5eGFP male mice after 8 weeks. Scale bars, 50 μ m.

Quantitative real-time RT-PCR confirmed the loss of expression of LGR5 mRNA in obese wild-type mice compared to lean counterparts. These data correlate with a recent report of dramatic loss of LGR5 expression in inflamed corneal cells and suggest a depletion of fast-cycling stem cells in the chronically inflamed state associated with obesity⁴⁶.

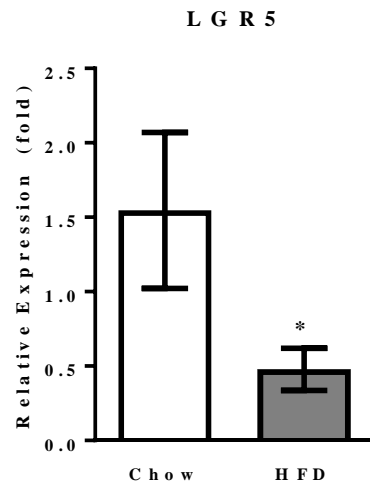
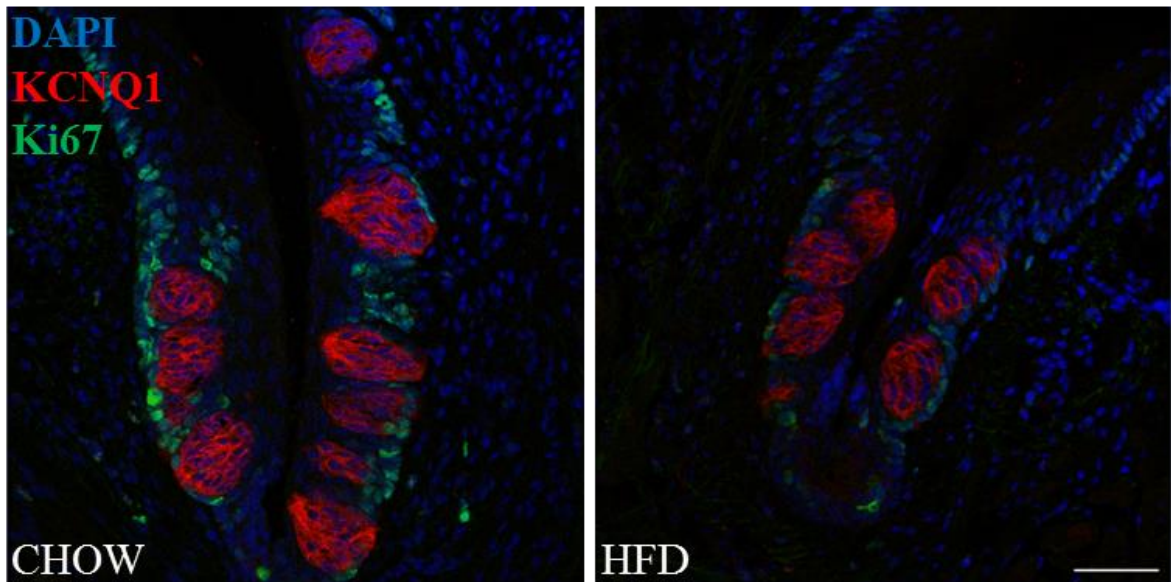


Figure 8: Loss of LGR5 mRNA expression in obese WT mice. Quantitative real-time PCR analysis of the expression of taste cell stem cell marker LGR5 in circumvallate papillae (CV) after 8-week treatment with chow and HFD (n=6 each). Error bars represent SEM. * $p < 0.05$; ** $p < 0.01$; *** $p < 0.005$.

Studies suggest that taste bud cells, as well as surrounding non-taste epithelial cells are derived from a pool of multipotent progenitor cells that exist in the basal regions surrounding taste buds^{32,33,45,47}. To investigate whether diet-induced obesity suppresses proliferation of taste bud progenitor cells, I performed immunostaining using antibodies against Ki67, an important marker for actively proliferating cells in the lingual epithelium³⁵ (Figure 8A), highlighting cells located in the basal periphery of adult taste buds, considered the niche for taste progenitor cells.

Obese mice exhibited fewer cells immunoreactive for Ki67. Sections were also stained for KCNQ1 to reveal the location of taste buds, with only Ki67 immunoreactive cells in contact with taste buds counted in quantification³⁵ (Figure 8B).

A



B

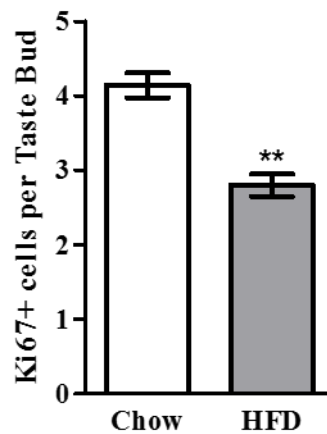


Figure 8: Loss of taste bud progenitor cell populations in obese WT mice. Confocal fluorescent images of circumvallate papillae stained with antibodies against KCNQ1 (red) and Ki67 (green) from chow and HFD-fed WT male mice after 8 weeks, with DAPI staining for nuclei (blue). (D) The number of Ki67-labeled cells per taste bud in circumvallate epithelium.

Only the Ki67-labeled cells that were adjacent to taste buds were counted. Obesity reduced the staining intensity and the number of cells labeled with Ki67 antibody (n=3 each). Error bars represent SEM. * p < 0.05; ** p < 0.01; *** p < 0.005. Scale bars, 50 μ m.

Quantitative RT-PCR confirmed the loss of Ki67 immunoreactivity, showing a significant decrease in the expression level of Ki67 mRNA in circumvallate papillae (Figure 9). The mRNA expression of beta-catenin (Figure 9), which is an important determinant of cell fate in taste bud development and is required for renewal of all three adult taste cell types was also notably decreased in the taste buds of obese mice⁴⁸. Low beta-catenin expression drives the differentiation of LGR5⁺ stem cells into keratinized epithelial cells surrounding taste buds, but not taste cells themselves, which could explain the gradual loss of adult taste buds I see in obese mice without damage to the overall morphology of the gustatory tissues⁴⁷.

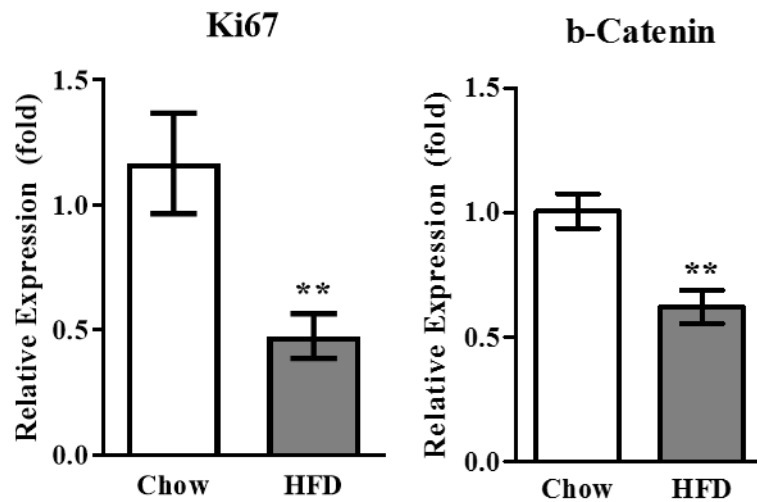


Figure 9: Loss of expression of key proliferative markers in taste buds of obese WT mice. Quantitative real-time PCR analysis of the expression of Ki67 and β catenin in circumvallate papillae (CV) after 8-week treatment with chow and HFD (n=6 each). Relative gene expression levels are shown (fold change). β -actin was used as the endogenous control gene for relative quantification. Error bars represent SEM. * p < 0.05; ** p < 0.01; *** p < 0.005.

Deletion of TNF α protects taste buds from obesity

TNF α expression is highly upregulated in obese wild-type mice, compared to lean controls (Figure 3). In order to determine if TNF α was necessary to cause the dysfunction in taste bud renewal obese mice exhibit, I employed the same dietary treatment previously described to two cohorts of 8-week-old B6.129S-Tnf^{tm1Gkl}/J male mice (Figure 10A). These TNF α -null mice are slightly smaller in size than wild-type mice at sexual maturity, but gained a similar percentage of their body weight on either diet, when compared to wild-type mice (Figure 10B), suggesting that deletion of TNF α did not impede adipogenesis resulting from HFD-feeding.

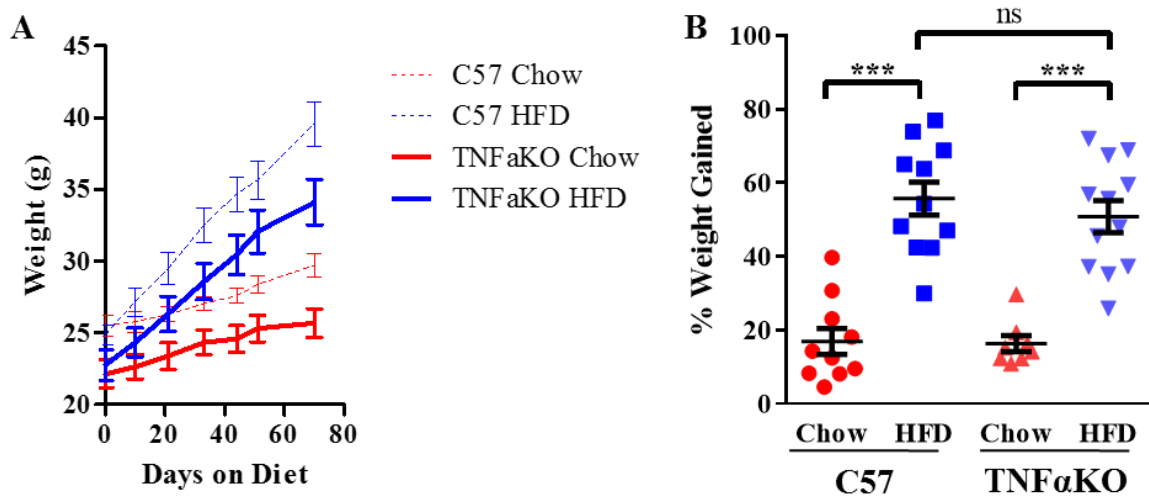


Figure 10: High fat diet induces significant adipogenesis in male TNF α -knockout mice similar to WT mice. (A) Growth curve of TNF α KO vs. WT mice over 8-weeks ad libitum feeding with standard chow and high fat diet (HFD). (B) Percentage weight gained by TNF α KO vs. WT mice after 8-week treatment period of standard chow and HFD (n=8,12 for TNF α KO). Error bars represent SEM. * p < 0.05; ** p < 0.01; *** p < 0.005.

Immunostaining and taste bud counting from circumvallate papillae sections of lean and obese TNF α -null mice did not reveal a reduction in taste bud abundance such as that seen in obese wild-type mice (Figure 11).

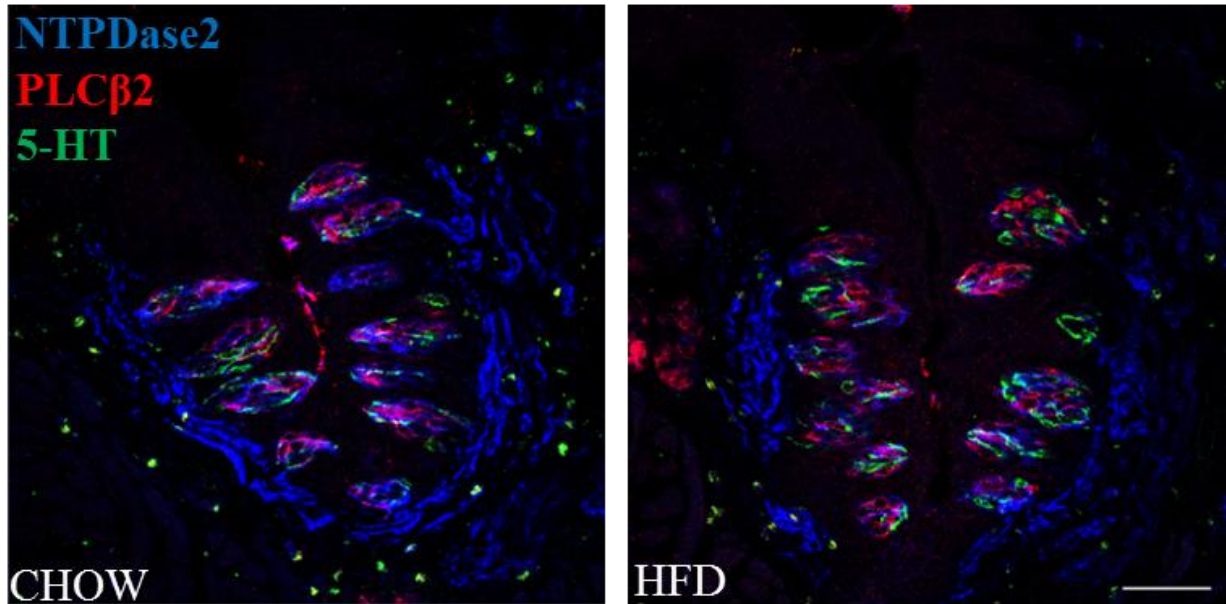


Figure 11: No loss of taste buds in TNF α -null mice. Confocal fluorescent images of circumvallate papillae stained with antibodies against NTPDase2 (blue), PLC β 2 (red), and 5-HT (green) from chow and HFD-fed TNF α KO mice after 8 weeks. Scale bars, 50 μ m.

The total number of taste buds in the circumvallate papillae of lean TNF α -null mice was slightly less than lean wild-type mice, as would be expected due to their smaller overall size. Taste bud area was also unaffected by diet in TNF α -null mice (Figure 12A, B).

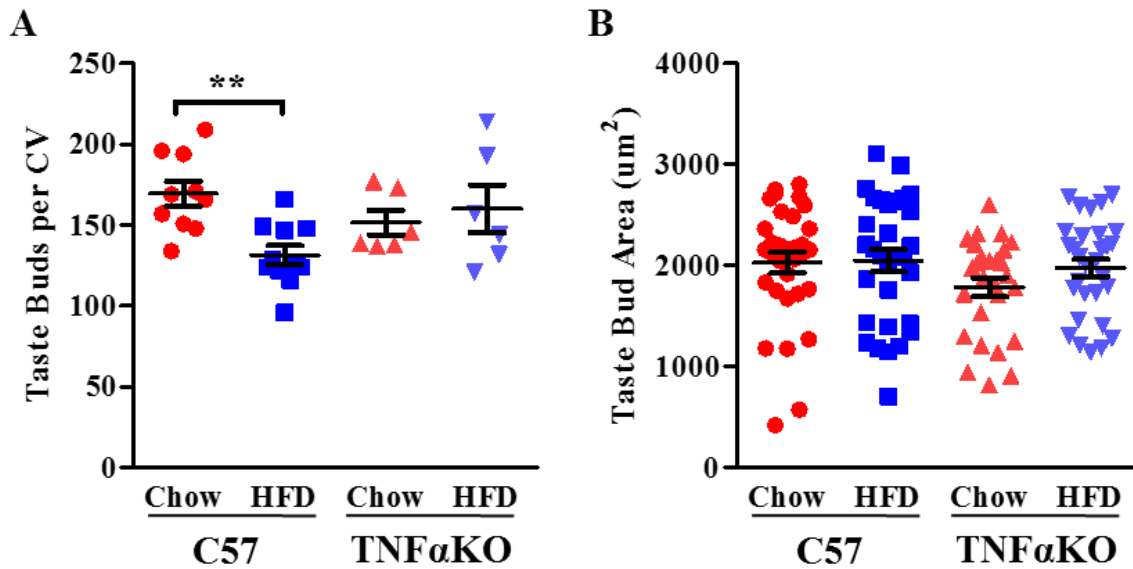


Figure 12: High fat diet does not reduce taste bud abundance in TNF α -null mice as it does in WT mice Total numbers of taste buds in circumvallate papillae of chow and HFD-fed WT vs. TNF α KO mice after 8 weeks (n=6 each for TNF α KO). (E) Taste bud area measurements from chow and HFD-fed WT vs. TNF α KO mice after 8 weeks (n=27, 31 for TNF α KO). Error bars represent SEM. * p < 0.05; ** p < 0.01; *** p < 0.005.

Quantitative real-time RT-PCR for KCNQ1, as well as taste markers NTPDase2, PLC β 2, and T1R3 showed no decrement in obesity, but rather was slightly higher in obese mice, compared to lean controls (Figure 13). This suggests the existence of a compensatory anti-inflammatory mechanism that co-exists with pro-inflammatory pathways in the obese state, possibly related to the observations of Feng et al³⁸.

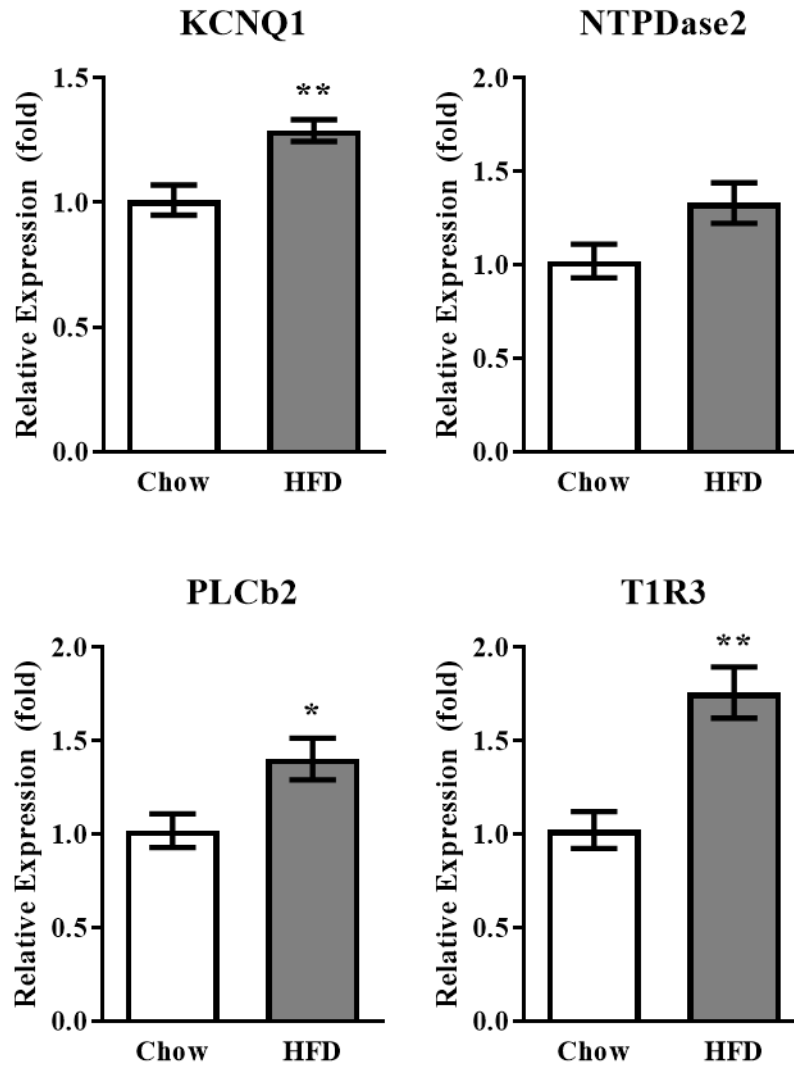
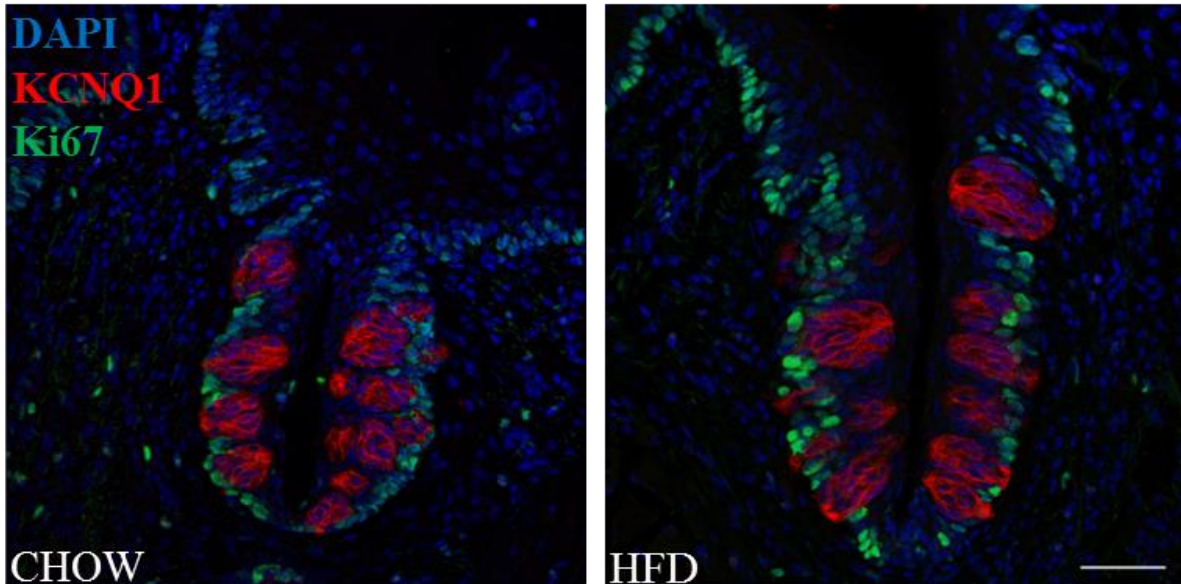


Figure 13: High fat diet does not cause loss of taste transduction machinery in TNF α -null mice. Quantitative real-time PCR analysis of the expression of taste cell markers in circumvallate papillae (CV) of TNF α KO mice after 8-week treatment with chow and HFD (n=3 each). Relative gene expression levels are shown (fold change). β -actin was used as the endogenous control gene for relative quantification. Error bars represent SEM. * $p < 0.05$; ** $p < 0.01$; *** $p < 0.005$.

Similar results were seen following immunostaining for Ki67 in TNF α -null mice. Obese mice did not experience the reduction in abundance of Ki67⁺ taste progenitor cells demonstrated in obese wild-type mice (Figure 14A, B).

A



B

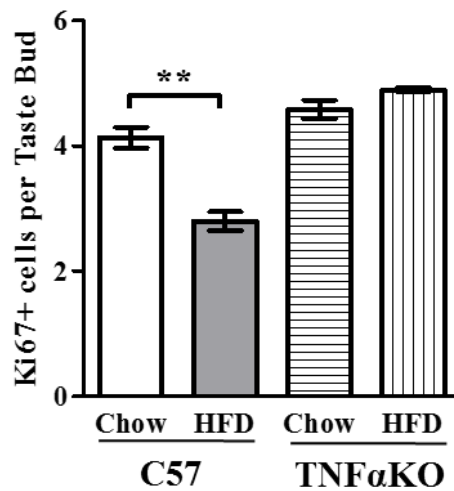


Figure 14: No loss of taste stem/progenitor cell populations in obese TNF α KO mice. (A) Confocal fluorescent images of circumvallate papillae stained with antibodies against KCNQ1 (red) and Ki67 (green) from chow and HFD-fed TNF α KO mice after 8 weeks. (B) The number of Ki67-labeled cells per taste bud in circumvallate epithelium in WT vs. TNF α KO mice. Only the Ki67-labeled cells that were adjacent to taste buds were counted. Obesity reduced the staining intensity and the number of cells labeled with Ki67 antibody in WT, but not TNF α KO mice (n=3 each). Error bars represent SEM. * p < 0.05; ** p < 0.01; *** p < 0.005.

Similar to overall taste bud quantification, the number of Ki67⁺ cells per taste bud slightly increased, as did expression of LGR5 and beta-catenin in quantitative RT-PCR analysis (Figure 15).

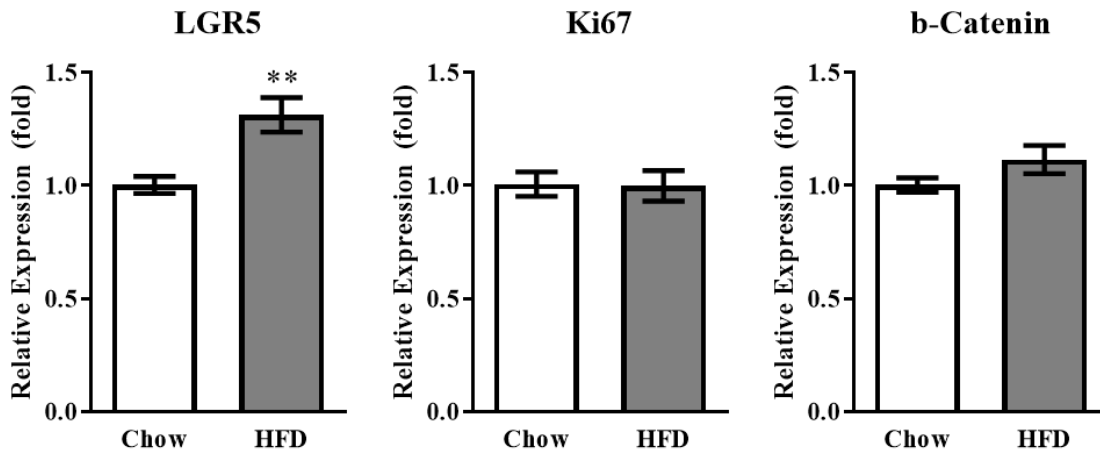
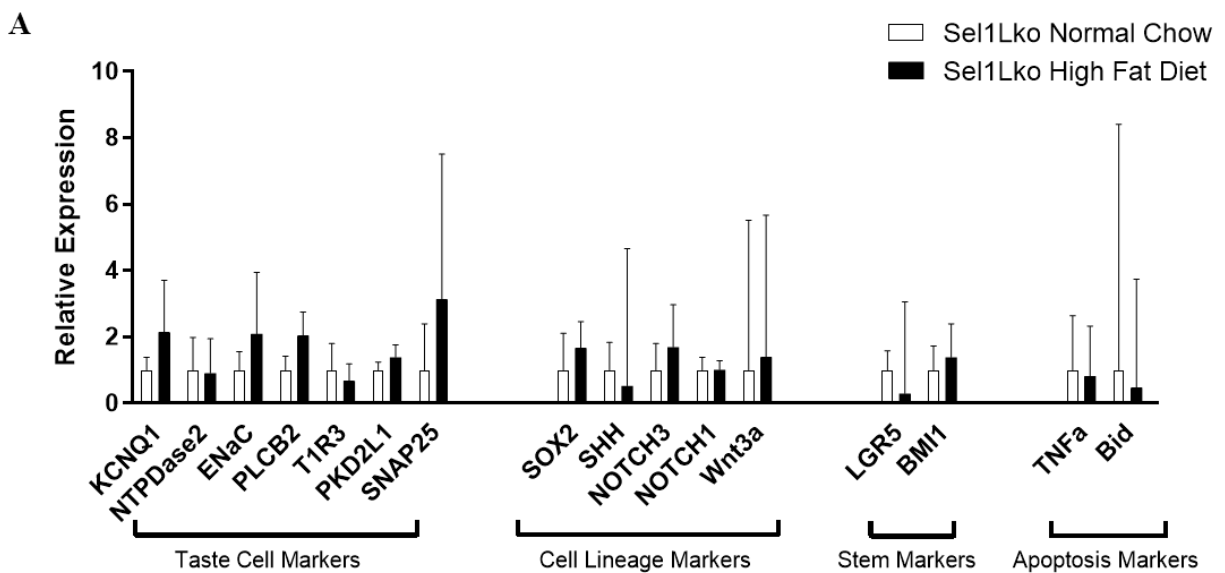


Figure 15: Quantitative real-time PCR analysis of the expression of LGR5, Ki67 and β -catenin in circumvallate papillae (CV) of TNF α KO mice after 8-week treatment with chow and HFD (n=3 each). Relative gene expression levels are shown (fold change). β -actin was used as the endogenous control gene for relative quantification. Error bars represent SEM. * p < 0.05; ** p < 0.01; *** p < 0.005. Scale bars, 50 μ m.

To determine whether a reduction in taste buds, taste proliferative capacity, or inflammatory response itself stemmed from the adiposity of the animals or the chronic oral exposure to the high-fat diet, gene expression analysis and immunostaining experiments were repeated in an obesity-resistant transgenic mouse model. Adipocyte-specific deletion of *Sel1L* results in inefficient metabolism of fatty acids and significantly reduced adiposity when maintained on a high-fat diet⁴⁹. These animals were subjected to the same dietary treatments as wild-type mice, and ate a similar amount of chow or HFD to wild-type mice, but did not show an increase in expression of TNF α after 8 weeks. Furthermore, expression of taste bud machinery and markers

of self-renewal were similarly unaffected in these mice (Figure 16A). Representative images of circumvallate papillae from chow and HFD-fed Adipo-Sel1L-knockout mice immunostained with antibodies against NTPDase2, PLC β 2, and 5-HT to reveal mature type I, type II and type III taste cells respectively also show no difference between dietary treatments, as with TNF α -null mice (Figure 16B). This would imply that the metabolic effects of obesity trigger a decline in taste, and not merely the oral exposure to fat.



B

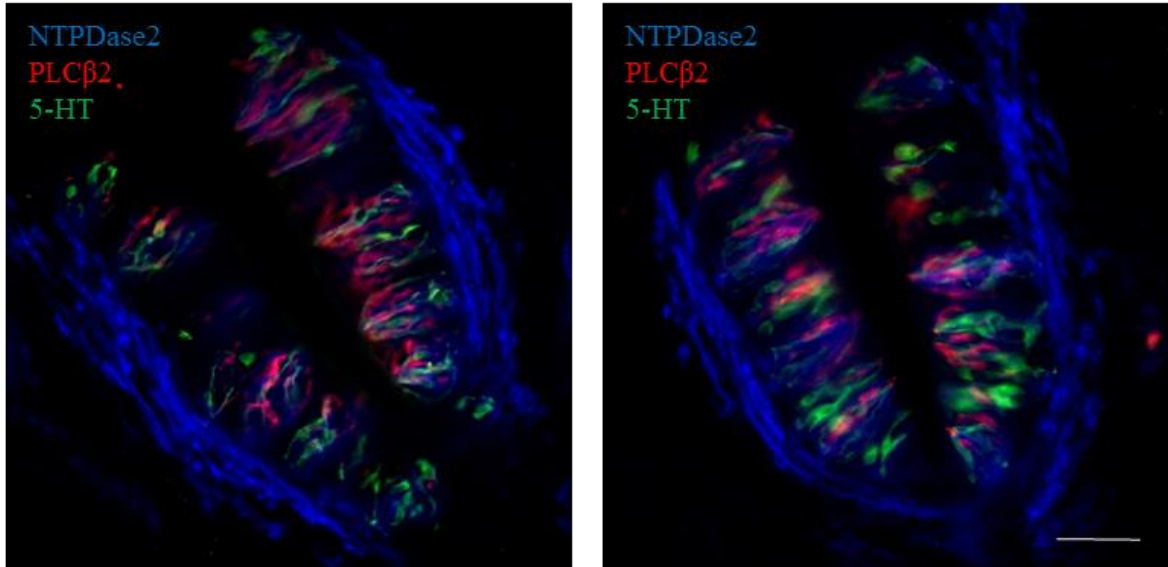


Figure 16: No taste machinery loss in obesity-resistant Adipocyte-specific-Sel1L knockout mice. (A) Quantitative real-time PCR analysis of the expression of markers of adult taste cells, development/stem cells, and inflammation in circumvallate papillae (CV) of obesity-resistant male mice after 8-week treatment with chow and HFD. Relative gene expression levels are shown (fold change). β -actin was used as the endogenous control gene for relative quantification. Error bars represent SEM (n=3, for each). (B) Confocal fluorescent images of circumvallate papillae stained with antibodies against NTPDase2 (blue), PLC β 2 (red), and 5-HT (green) from chow and HFD-fed obesity-resistant male mice after 8 weeks. Scale bars, 50 μ m.

All of these data together suggest that gross adiposity stemming from chronic exposure to a high-fat diet, is associated with a low-grade inflammatory response causing a disruption in the homeostatic mechanisms of taste bud maintenance and renewal. Inhibition of proinflammatory cascades, whether by genetic deletion of TNF α or by resistance to adipogenesis, is sufficient to avert the systematic loss of taste buds due to an obesogenic diet, and may highlight novel therapeutic targets in the alleviation of taste dysfunction in obese populations.

Materials and Methods

Animals

C57BL/6 and B6.129S-Tnf^{tm1Gkl}/J mice were purchased from Jackson Laboratory (Bar Harbor, ME). B6.129P2-Lgr5^{tm1(cre/ERT2)Cle}/J mice were a gift from Dr. Xiling Shen of Duke University. Adipocyte-specific Sell^{L^{-/-}} (AKO) mice were a gift from Dr. Ling Qi of the University of Michigan Medical School. Mice were housed in a climate-controlled environment at the East Campus Research Facility at Cornell University College of Veterinary Medicine. 8 week old male mice were fed on either standard rodent diet consisted of 14% fat, 54% carbohydrate, and 32% protein (Harlan Teklad 8604) or a high fat diet consisted of 58.4% fat, 26.6% carbohydrate, and 15% protein (Harlan Teklad TD.03584) for a period of 8 weeks. Mice were sacrificed by exposure to CO₂ followed by cervical dislocation. Inguinal and epididymal white adipose tissue depots were excised and weighed postmortem. Studies were performed according to protocols approved by the Cornell University Institutional Animal Care and Use Committee.

Quantitative real-time RT-PCR

Following dietary treatment, mice were sacrificed and tongues were incubated in ice cold normal Tyrode's solution (NaCl 135mM, KCl 5mM, CaCl₂ 2mM, MgCl 1mM, NaHCO₃ 5mM, HEPES 10mM, Glucose 10mM, Sodium Pyruvate 10mM, pH 7.4). The excised tongue was injected subepithelially with a mixture of Dispase II (2.5mg/ml), Collagenase A (1mg/ml), Elastase (0.25mg/ml), and DNaseI (0.5mg/ml) in Tyrode's solution and incubated at room temp for 20 minutes. Epithelial sections containing taste buds and non-taste epithelial control tissues were collected and total RNA extracted using Absolutely RNA Microprep Kit (Stratagene, Cedar

Creek, TX). Samples were reverse transcribed into cDNA using qScript cDNA Supermix (Quanta Bio, Beverly, MA). Quantitative real-time PCR using Power SYBR Green PCR Master Mix (Applied Biosystems) was run on a QuantStudio 6 Flex Real-Time PCR System (Thermo). Relative quantification was performed using QuantStudio PCR Software, based on the $2^{-\Delta\Delta Ct}$ method. β Actin was used as an endogenous housekeeping control gene for these analyses.

Taste Bud Counting and Size measurement

Mice were sacrificed and tongues were removed and fixed in 4% PFA/PBS solution. Tissues were cryosectioned at 10um thickness and washed in PBS. Circumvallate sections were incubated in blocking buffer (2% bovine serum albumin, 0.3% Triton X-100, 2% donkey serum) at room temperature for 2 hours. The sections were then incubated in polyclonal goat antibody against KCNQ1 at 4°C overnight. The sections were washed 3X in PBS and further incubated in AlexaFluor 647-conjugated donkey anti-goat secondary antibody at room temperature for 2 hours. Sections were washed 3X in PBS and mounted with ProLong Gold mounting medium containing DAPI. Images were taken using an Olympus IX71 Inverted Fluorescent Microscope. Taste buds were imaged using ImageJ and counted from every 5th section to avoid double counting. To calculate taste bud size, the perimeter of the largest taste bud (from every 5th section) was outlined and the corresponding area was calculated using ImageJ⁵⁰.

Taste Bud Cell Type staining

Mice were sacrificed and tongues were removed and fixed in 4% PFA/PBS solution. Tissues were cryosectioned at 10um thickness and washed in PBS. Circumvallate sections were incubated in blocking buffer (2% bovine serum albumin, 0.3% Triton X-100, 2% donkey serum)

at room temperature for 2 hours. The sections were then incubated in a mixture of polyclonal goat antibody against PLC β 2 (Santa Cruz #sc-31759, 1:1000), rat polyclonal antibody against 5HT (Millipore #MAB352, 1:1000), and rabbit monoclonal antibody against NTPDase2 (Sevigny lab, CHU de Québec, #mN2-36I6, 1:500) at 4°C overnight. The sections were washed 3X in PBS and further incubated in AlexaFluor 647-conjugated donkey anti-goat secondary antibody at room temperature for 2 hours. Sections were washed 3X in PBS and mounted with Prolong Gold medium containing DAPI. Images were taken using a Zeiss LSM710 confocal microscope.

Ki67 Immunostaining and cell counting

Mice were sacrificed and tongues were removed and fixed in 4% PFA/PBS solution. Tissues were cryosectioned at 10 μ m thickness and washed in PBS. Circumvallate sections were washed in methanol + 3% hydrogen peroxide for 30 minutes and then rinsed 3X in PBS. Sections were incubated in blocking solution (2% bovine serum albumin, 0.3% Triton X-100, 2% donkey serum) for 2 hours and then further incubated overnight at 4°C with antibodies against KCNQ1 (Santa Cruz #sc-10646, 1:1000) and Ki67 (Thermo Scientific #RM-9106-S1, 1:200). After washing 3X with PBS, the sections were incubated with AlexaFluor 647-conjugated anti-goat secondary (for KCNQ1) and AlexaFluor 488-conjugated anti-rabbit secondary (for Ki67) at room temperature for 2 hours. Sections were washed and mounted with ProLong Gold mounting media. Images of every 5th section were taken with a Zeiss LSM710 confocal microscope. Only Ki67-labeled cells immediately surrounding a taste bud (defined by the KCNQ1 staining) were counted. The average number of taste Ki67-positive cells per taste bud were calculated for both standard chow and HFD-fed mice.

REFERENCES

1. Flegal, K. M., Carroll, M. D., Ogden, C. L. & Curtin, L. R. CLINICIAN ' S CORNER Among US Adults , 1999-2008. *J. Am. Med. Assoc.* **303**, 235–241 (2013).
2. Allison, D. B., Fontaine, K. R., Manson, J. E., Stevens, J. & VanItallie, T. B. Annual Deaths Attributable to Obesity in the United States. *Jama* **282**, 1530–1538 (1999).
3. Colombo, O. *et al.* Is drop-out from obesity treatment a predictable and preventable event? *Nutr. J.* **13**, 13 (2014).
4. Grinker, J., Hirsch, J. & Smith, D. V. Taste sensitivity and susceptibility to external influence in obese and normal weight subjects. *J. Pers. Soc. Psychol.* **22**, 320–325 (1972).
5. Thompson, D. A., Moskowitz, H. R. & Campbell, R. G. *Taste and olfaction in human obesity. Physiology & Behavior* **19**, (1977).
6. Bartoshuk, L. . *et al.* Valid across-group comparisons with labeled scales: the gLMS versus magnitude matching. *Physiol. Behav.* **82**, 109–114 (2004).
7. Bartoshuk, L. M. *et al.* Psychophysics of sweet and fat perception in obesity: problems, solutions and new perspectives. *Philos. Trans. R. Soc. Lond. B. Biol. Sci.* **361**, 1137–48 (2006).
8. Sartor, F. *et al.* Taste perception and implicit attitude toward sweet related to body mass index and soft drink supplementation. *Appetite* **57**, 237–246 (2011).
9. Skrandies, W. & Zschieschang, R. Olfactory and gustatory functions and its relation to body weight. *Physiol. Behav.* **142**, 1–4 (2015).
10. Pepino, M. Y., Finkbeiner, S., Beauchamp, G. K. & Mennella, J. A. Obese Women Have Lower Monosodium Glutamate Taste Sensitivity and Prefer Higher Concentrations Than Do Normal-weight Women. *Obesity* **18**, 959–965 (2010).

11. Davis, C., Strachan, S. & Berkson, M. Sensitivity to reward: implications for overeating and overweight. *Appetite* **42**, 131–138 (2004).
12. Wang, Y. C., McPherson, K., Marsh, T., Gortmaker, S. L. & Brown, M. Health and economic burden of the projected obesity trends in the USA and the UK. *Lancet* **378**, 815–825 (2011).
13. Bueter, M. *et al.* Alterations of sucrose preference after Roux-en-Y gastric bypass. *Physiol. Behav.* **104**, 709–721 (2011).
14. Burge, J. C., Schaumburg, J. Z., Choban, P. S., DiSilvestro, R. A. & Flancbaum, L. Changes in patients' taste acuity after Roux-en-Y gastric bypass for clinically severe obesity. *J. Am. Diet. Assoc.* **95**, 666–671 (1995).
15. Berthoud, H.-R., Zheng, H. & Shin, A. C. Food reward in the obese and after weight loss induced by calorie restriction and bariatric surgery. *Ann. N. Y. Acad. Sci.* **1264**, 36–48 (2012).
16. le Roux, C. W. *et al.* Gastric bypass reduces fat intake and preference. *Am. J. Physiol. Regul. Integr. Comp. Physiol.* **301**, R1057–66 (2011).
17. Pepino, M. Y. *et al.* Changes in taste perception and eating behavior after bariatric surgery-induced weight loss in women. *Obesity* **22**, E13–E20 (2014).
18. Scruggs, D. M., Buffington, C. & Cowan Jr., G. S. M. Taste Acuity of the Morbidly Obese before and after Gastric Bypass Surgery. *Obes. Surg.* **4**, 24–28 (1994).
19. Thanos, P. K. *et al.* Roux-en-Y Gastric Bypass Alters Brain Activity in Regions that Underlie Reward and Taste Perception. *PLoS One* **10**, e0125570 (2015).
20. Umabiki, M. *et al.* The Improvement of Sweet Taste Sensitivity with Decrease in Serum Leptin Levels During Weight Loss in Obese Females. *Tohoku J. Exp. Med.* **220**, 267–271 (2010).
21. Chandrashekar, J. *et al.* The cells and peripheral representation of sodium taste in mice. *Nature* **464**, 297–301 (2010).

22. Mueller, K. L. The receptors and coding logic for bitter taste. **434**, 7030–225 (2005).
23. Liu, D. & Liman, E. R. Intracellular Ca²⁺ and the phospholipid PIP₂ regulate the taste transduction ion channel TRPM5. *Proc. Natl. Acad. Sci.* **100**, 15160–15165 (2003).
24. Zhao, G. Q. *et al.* The Receptors for Mammalian Sweet and Umami Taste. *Cell* **115**, 255–266 (2003).
25. Huang, Y. A., Maruyama, Y., Stimac, R. & Roper, S. D. Presynaptic (Type III) cells in mouse taste buds sense sour (acid) taste. *J. Physiol.* **586**, 2903–2912 (2008).
26. Yang, R., Crowley, H. H., Rock, M. E. & Kinnamon, J. C. Taste cells with synapses in rat circumvallate papillae display SNAP-25-like immunoreactivity. *J. Comp. Neurol.* **424**, 205–215 (2000).
27. Huang, Y.-J. *et al.* The role of pannexin 1 hemichannels in ATP release and cell-cell communication in mouse taste buds. *Proc. Natl. Acad. Sci.* **104**, 6436–6441 (2007).
28. Dando, R. & Roper, S. D. Acetylcholine is released from taste cells, enhancing taste signalling. *J. Physiol.* **590**, 3009–3017 (2012).
29. Huang, Y. A., Pereira, E. & Roper, S. D. Acid Stimulation (Sour Taste) Elicits GABA and Serotonin Release from Mouse Taste Cells. *PLoS One* **6**, e25471 (2011).
30. Perea-Martinez, I. *et al.* Functional Cell Types in Taste Buds Have Distinct Longevities. *PLoS One* **8**, e53399 (2013).
31. Barker, N. *et al.* Identification of stem cells in small intestine and colon by marker gene Lgr5. doi:10.1038/nature06196
32. Takeda, N. *et al.* Lgr5 Identifies Progenitor Cells Capable of Taste Bud Regeneration after Injury. *PLoS One* **8**, e66314 (2013).
33. Yee, K. K. *et al.* Lgr5-EGFP Marks Taste Bud Stem/Progenitor Cells in Posterior Tongue. *Stem Cells* **31**, 992–1000 (2013).

34. Okubo, T., Pevny, L. H. & Hogan, B. L. M. Sox2 is required for development of taste bud sensory cells. *Genes Dev.* **20**, 2654–2659 (2006).
35. Cohn, Z. J. *et al.* Lipopolysaccharide-induced inflammation attenuates taste progenitor cell proliferation and shortens the life span of taste bud cells. *BMC Neurosci.* **11**, 72 (2010).
36. Hotamisligil, G. S. Inflammation and metabolic disorders. *Nature* **444**, 860–867 (2006).
37. Shoelson, S. E. Inflammation and insulin resistance. *J. Clin. Invest.* **116**, 1793–1801 (2006).
38. Feng, P. *et al.* Interleukin-10 Is Produced by a Specific Subset of Taste Receptor Cells and Critical for Maintaining Structural Integrity of Mouse Taste Buds. *J. Neurosci.* **34**, 2689–2701 (2014).
39. Feng, P. *et al.* Regulation of bitter taste responses by tumor necrosis factor. *Brain Behav. Immun.* **49**, 32–42 (2015).
40. Hall, J. M. ., Bell, M. L. & Finger, T. E. Disruption of sonic hedgehog signaling alters growth and patterning of lingual taste papillae. *Dev. Biol.* **255**, 263–277 (2003).
41. Miller, I. J. & Reedy, F. E. Variations in human taste bud density and taste intensity perception. *Physiol. Behav.* **47**, 1213–1219 (1990).
42. Wang, H. *et al.* Expression of the voltage-gated potassium channel KCNQ1 in mammalian taste bud cells and the effect of its null-mutation on taste preferences. *J. Comp. Neurol.* **512**, 384–398 (2009).
43. Herrera Moro Chao, D. *et al.* Impact of obesity on taste receptor expression in extra-oral tissues: emphasis on hypothalamus and brainstem. *Sci. Rep.* **6**, 29094 (2016).
44. Ren, W. *et al.* Single Lgr5- or Lgr6-expressing taste stem/progenitor cells generate taste bud cells ex vivo. *Proc. Natl. Acad. Sci.* **111**, 16401–16406 (2014).

45. Feng, P., Huang, L. & Wang, H. Taste bud homeostasis in health, disease, and aging. *Chem. Senses* **39**, 3–16 (2014).
46. Curcio, C., Lanzini, M., Calienno, R., Mastropasqua, R. & Marchini, G. The expression of LGR5 in healthy human stem cell niches and its modulation in inflamed conditions. *Mol. Vis.* **21**, 644–8 (2015).
47. Gaillard, D. *et al.* β -Catenin Signaling Biases Multipotent Lingual Epithelial Progenitors to Differentiate and Acquire Specific Taste Cell Fates. *PLoS Genet.* **11**, e1005208 (2015).
48. Gaillard, D. & Barlow, L. A. Taste bud cells of adult mice are responsive to Wnt/ β -catenin signaling: Implications for the renewal of mature taste cells. *genesis* **49**, 295–306 (2011).
49. Sha, H. *et al.* The ER-associated degradation adaptor protein SellL regulates LPL secretion and lipid metabolism. *Cell Metab.* **20**, 458–70 (2014).
50. Nosrat, I. V., Margolskee, R., & Nosrat, C. A. (2012). Targeted taste cell specific overexpression of BDNF in adult taste buds elevates pTrkB levels in taste cells, increases taste bud size and promotes gustatory innervation. *Journal of Biological Chemistry*, **287**(20), 16791-16800.